Bull. Chem. Soc. Jpn., 71, 2267—2279 (1998)

Headline Articles

Thermodynamic Study on Dioxygen Binding of Diiron(II) and Dicobalt(II) Complexes Containing Various Dinucleating Ligands

Hideki Sugimoto, Toshihiko Nagayama, Sachihito Maruyama, Shuhei Fujinami, Yuichi Yasuda, Masatatsu Suzuki,* and Akira Uehara*

Department of Chemistry, Faculty of Science, Kanazawa University, Kanazawa 920-1192

(Received March 30, 1998)

A new dinucleating ligand containing a sterically bulky imidazolyl group, Ph-Htidp (*N,N,N′,N′*-tetrakis[(1-methyl-4,5-diphenyl-2-imidazolyl)methyl]-1,3-diamino-2-propanol), and its μ-alkoxo-diiron(II) complexes $[Fe_2(Ph\text{-}tidp)(RCO_2)](ClO_4)_2$, ($RCO_2 = C_6H_5CO_2$ (**1**), $C_6F_5CO_2$ (**2**), CF_3CO_2 (**3**), and $C_2H_5CO_2$ (**4**)), were synthesized. The structure of complex **1** was determined by X-ray crystallography. Complex **1** crystallizes in the monoclinic space group $P2_1/c$ with $a = 13.464(2)$, $b = 19.223(4)$, $c = 31.358(4)$ Å, $\beta = 92.84(2)°$, and $Z = 4$. The complex has a doubly-bridged structure with μ-alkoxo of Ph-tidp and μ-benzoate; the two iron centers have a distorted five-coordinate structure with N_3O_2 donor set. All the complexes showed fairly good reversible oxygenation below −30 °C in CH_2Cl_2, which was monitored by UV-vis and NMR spectroscopies, and dioxygen up-take measurements. Introduction of 4,5-diphenyl substituents into 2-imidazolyl group stabilized the μ-peroxo diiron species against irreversible oxidation, just as introduction of 6-methyl substituent into 2-pyridyl group did. Phenyl substituents appear to weaken the electron donor ability of a dinucleating ligand to stabilize divalent oxidation state of iron and to form a hydrophobic cavity for a O_2 binding site, which would suppress the irreversible oxidation and facilitate the reversible oxygenation. Dioxygen affinities of the Ph-tidp and Me_4-tpdp diiron(II), and the tpdp and bpmp dicobalt(II) complexes were measured, $[Fe_2(Me_4\text{-}tpdp)(RCO_2)]^{2+}$ ($RCO_2 = C_6H_5CO_2$ and $RCO_2 = CF_3CO_2$) and $[Co_2(L)(RCO_2)]^{2+}$ (L = tpdp, $RCO_2 = CH_3CO_2$, and L = bpmp, $RCO_2 = C_6F_5CO_2$, and CF_3CO_2), where Me_4-tpdp, tpdp, and bpmp are *N,N,N′,N′*-tetrakis[(6-methyl-2-pyridyl)methyl]-1,3-diamino-2-propanolate, *N,N,N′,N′*-tetrakis(2-pyridylmethyl)-1,3-diamino-2-propanolate, and 2,6-bis[bis(2-pyridylmethyl)aminomethyl]-4-methylphenolate, respectively. Within a series of the Ph-tidp diiron(II) complexes, dioxygen affinity is well correlated with electron donor ability of bridging carboxylates (**1** ($C_6H_5CO_2$) > **2** ($C_6F_5CO_2$) > **3** (CF_3CO_2)). In contrast to the above trend, dioxygen affinities of the Ph-tidp complexes are lower than those of the Me_4-tpdp complexes, although electron donor abilities of the Me_4-tpdp complexes are weaker than those of the Ph-tidp complexes. Significant enhancement of dioxygen affinity was observed for both iron and cobalt complexes with 2,6-bis(aminomethyl)phenolate bridging skeleton compared to the complexes with a 1,3-diamino-2-propanolate bridging one. Thermodynamic study suggested that the observed enhancement is mainly attributable to a favorable entropy effect along with a steric effect.

Chemistry of diiron-dioxygen complexes[1] is of particular importance to gain insight into the structures and functions of diiron centers of hemerythrin (Hr),[2] ribonucleotide reductase (RNR),[3] and methane monooxygenase (MMO).[4] The role of Hr is a dioxygen transporter and it binds O_2 reversibly in a hydroperoxo fashion. The diiron center of RNR R2 activates O_2 to oxidize tyrosine to tyrosine radical for DNA biosynthesis. MMO also activates O_2 to hydroxylate methane to methanol. Recently, a "*peroxo intermediate*" has been found as an intermediate of dioxygen activation by diiron center in MMOH.[5] Mechanism of dioxygen activation by MMOH has been proposed to involve a di(μ-oxo)diiron(IV, IV)species with a diamond core "*compound Q*",[6] which is converted from a "*peroxo intermediate*".

The iron-dioxygen complexes have been shown to be highly susceptible to irreversible oxidation. Only a few iron(II) complexes that bind O_2 in a μ-peroxo fashion have been known.[7—12] In order to suppress such irreversible oxidation of iron(II) ion, we have developed various dinucleating ligands with sterically bulky nitrogen bases (6-methyl-2-pyridyl or 4,5-diphenyl-2-imidazolyl group) as shown in Scheme 1.[9,10] These sterically bulky ligands are effective to prevent the irreversible oxidation of iron(II) complexes by dioxygen. A similar observation was made for $[Fe_2(C_6H_5CO_2)(HB(3,5\text{-}iPr_2pz)_3)]_2(O_2)$ (**13**)[13] by Kitajima et al.[7] We have also found that dioxygen affinity of diiron(II) and dicobalt(II) complexes is highly dependent on stereochemistry of the dinucleating ligands.[14] For example, $P_{1/2}$

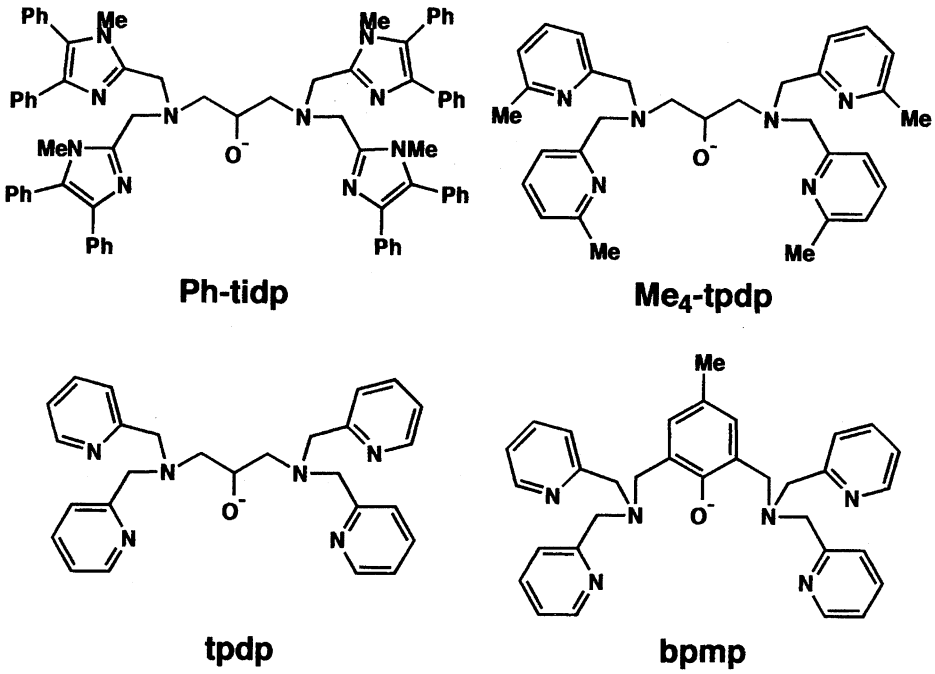

Scheme 1. Dinucleating ligands.

of $[Fe_2(Ph\text{-}bimp)(C_6H_5CO_2)]^{2+}$ (**14**) (ca. 2 Torr at 20 °C, 1 Torr = 133.322 Pa)[10] is much higher than that of the Me_4-tpdp complex (ca. 2 Torr at −40 °C) and comparable to that of Hr (ca. 2 Torr at 20 °C),[15] where $P_{1/2}$ ($= 1/K$) is a dioxygen partial pressure at which half of the total amount of the complex is oxygenated. As our current studies on the correlation between the stereochemistry of the dinucleating ligands and the dioxygen affinity, we measured dioxygen affinity of a series of diiron(II) and dicobalt(II) complexes with various dinucleating ligands, which have a significant influence on the dioxygen affinity.

Experimental

Materials. Acetonitrile, DMSO, and DMF were purified by refluxing with CaH_2 and distilled under N_2 atmosphere. Dichloromethane was purified by refluxing with P_2O_5 and distilled under N_2 atmosphere. All other chemicals were of reagent grade.

Syntheses of Ligands. Scheme 2 outlines the synthetic route of Ph-Htidp.

1-Methyl-4,5-diphenylimidazole (A). To a suspension of 4,5-diphenylimidazole[16] (213 g, 0.97 mol) in 500 cm^3 of THF was added NaH (26 g, 1.1 mol). The resulting blue green solution was stirred for 3 h; to this CH_3I (165 g, 1.2 mol) was added dropwise with stirring at 0 °C. After the solution was stirred overnight, the white powder which deposited was collected by filtration and washed with water, ethanol, and then ether. The white powder was recrystallized from chloroform/ether. Yield: 159 g (70%). Found: 82.04; 5.93; 12.04%. Calcd for $C_{16}H_{14}N_2$: C, 82.02; H, 6.02; N, 11.96%. ^{1}H NMR ($CDCl_3$, 400 MHz) δ = 3.49 (3H, s, CH_3), 7.12—7.50 (10H, m, Ph), 7.58 (1H, s, Im). MS *m/z* 234 [M^+].

1-Methyl-4,5-diphenylimidazole-2-carbaldehyde (B). To a suspension of **A** (30 g, 128 mmol) in 300 cm^3 of dry THF was added butyllithium (154 mmol) in hexane with stirring below −45 °C. After the resulting brown solution was stirred for 2 h, dry DMF (14 cm^3, 180 mmol) was added to the solution below −45 °C. After being stirred overnight at −45 °C and warmed to room temperature,

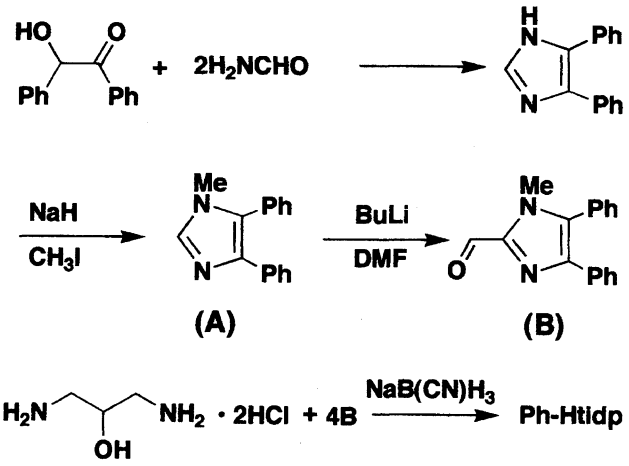

Scheme 2. Synthetic route for Ph-Htidp.

the reaction mixture was quenched by the addition of an aqueous solution saturated with NH_4Cl (300 mmol). The reaction mixture was condensed almost to dryness under reduced pressure and the residue was dissolved in chloroform, which was washed several times with water. The chloroform solution was dried over Na_2SO_4 and the solvent was removed under reduced pressure to give a brown powder. Recrystallization was carried out by dissolving it into a minimum amount of benzene and then adding ether. Yield: 25.3 g (75%). Found: 77.68; 5.33; 10.56%. Calcd for $C_{17}H_{14}N_2O$: C, 77.84; H, 5.38; N, 10.68%. ^{1}H NMR $CDCl_3$, 400 MHz) δ = 3.83 (3H, s, CH_3), 7.19—7.51 (10H, m, Ph), 9.92 (1H, s, CHO). MS *m/z* 262 [M^+].

***N,N,N′,N′*-Tetrakis[(1-methyl-4,5-diphenyl-2-imidazolyl)-methyl]-1,3-diamino-2-propanol (Ph-Htidp).** 1,3-Diamino-2-propanol dihydrochloride (1.9 g, 12 mmol) was dissolved in a small amount of water and thereto 150 cm^3 of methanol was added. To the resulting methanol solution was added **B** (6.0 g, 23 mmol). After the solution was stirred for two days, sodium cyanotrihydroborate (1.0 g, 16 mmol) was added to the solution. The solution was

then stirred for two days at room temperature. Additional **B** (6.0 g, 23 mmol) and sodium cyanotrihydridoborate (1.0 g, 16 mmol) were added to the solution in the same manner as that described above. The solution was stirred for two days, subsequently acidified by addition of concentrated hydrochloric acid, and evaporated almost to dryness under reduced pressure. The residue was taken up into a mixture of 4 M (1 M = 1 mol dm^{-3}) NaOH aqueous solution (100 cm^3) and chloroform (50 cm^3). After stirring for 2 h, the chloroform layer was separated and the aqueous layer was extracted with chloroform (2×50 cm^3). The combined extracts were dried over Na_2SO_4 and evaporated under reduced pressure to give yellow powder, which was purified by silica gel column chromatography with chloroform/methanol. Yield: 6.0 g (48%). Found: 73.74; 5.76; 12.36%. Calcd for $C_{71}H_{66}H_{10}O{\cdot}0.5CHCl_3{\cdot}1.5H_2O$: C, 73.90; H, 6.03; N, 12.05% (Presence of $CHCl_3$ was confirmed by ^{1}H NMR in CD_3OD). ^{1}H NMR ($CDCl_3$, 400 MHz) δ = 2.88 (4H, m, CH_2), 3.22 (12H, s, CH_3), 3.83 (1H, m, CH), 3.98 (8H, q, CH_2im), 4.82 (1H, s, OH), 7.06—7.43 (40H, m, Ph). MS *m/z* 1076 $[MH_2]^+$.

***N,N,N′,N′*-Tetrakis(2-pyridylmethyl)-1,3-diamino-2-propanol (Htpdp).** This was prepared as described elsewhere.[14d]

***N,N,N′,N′*-Tetrakis[(6-methyl-2-pyridyl)methyl]-1,3-diamino-2-propanol (Me$_4$-Htpdp).** This was prepared as described previously.[9b]

2,6-Bis[bis(2-pyridylmethyl)aminomethyl]-4-methylphenol (Hbpmp). This was prepared as described elsewhere.[14a]

Syntheses of Complexes. All the manipulations for preparation of the diiron(II) and dicobalt(II) complexes were carried out under N_2 atmosphere using Schlenk techniques. *Caution: Perchlorate salts are potentially explosive and should be handled with care.*

[Fe$_2$(Ph-tidp)(C$_6$H$_5$CO$_2$)](ClO$_4$)$_2$·CH$_3$CN·H$_2$O (1). To a stirred solution of Ph-Htidp (538 mg, 0.5 mmol), $C_6H_5CO_2H$ (61 mg, 0.5 mmol), and triethylamine (101 mg, 1.0 mmol) in 10 cm^3 of acetonitrile was added $Fe(ClO_4)_2{\cdot}6H_2O$ (363 mg, 1.0 mmol). The resulting yellowish brown solution was stirred for 10 min; then 20 cm^3 of ether was added. The mixture was allowed to stand overnight to give white crystals, which were collected by filtration, washed with methanol and ether, and dried in vacuo. Recrystallization from an acetonitrile/ether solution gave colorless crystals. Yield: 350 mg (45%). Found: C, 61.05; H, 5.13; N, 9.96%. Calcd for $Fe_2C_{80}H_{75}N_{11}Cl_2O_{12}$: C, 61.39; H, 4.83; N, 9.85% Molar conductivity (in acetonitrile, S mol^{-1} cm^2) 291. IR (KBr) ν_{as} (COO) 1548, ν_s (COO) 1415 cm^{-1}.

[Fe$_2$(Ph-tidp)(C$_6$F$_5$CO$_2$)](ClO$_4$)$_2$·2H$_2$O (2). The complex was prepared in the same way as that of **1** except for using $C_6F_5CO_2H$ instead of $C_6H_5CO_2H$. White needle crystals were obtained. Found: C, 57.65; H, 4.19; N, 8.60%. Calcd for $Fe_2C_{78}H_{69}N_{10}Cl_2F_5O_{13}$: C, 57.40; H, 4.26; N, 8.58%. Molar conductivity (S mol^{-1} cm^2) 267. IR (KBr) ν_{as}(COO) 1617, ν_s(COO) 1403 cm^{-1}.

[Fe$_2$(Ph-tidp)(CF$_3$CO$_2$)](ClO$_4$)$_2$·H$_2$O (3). The complex was prepared in the same way as that of **1** except for using CF_3CO_2H instead of $C_6H_5CO_2H$. Colorless needle crystals were obtained. Found: C, 57.41; H, 4.50; N, 9.34%. Calcd for $Fe_2C_{73}H_{67}N_{10}Cl_2F_3O_{12}$: C, 57.84; H, 4.45; N, 9.24%. Molar conductivity (S mol^{-1} cm^2) 242. IR (KBr) ν_{as}(COO) 1663, ν_s(COO) 1444 cm^{-1}.

[Fe$_2$(Ph-tidp)(C$_2$H$_5$CO$_2$)](ClO$_4$)$_2$·3H$_2$O (4). The complex was prepared in the same way as that of **1** except for using $C_2H_5CO_2H$ instead of $C_6H_5CO_2H$. Colorless needle crystals were obtained. Found: C, 58.69; H, 5.01; N, 9.24%. Calcd for $Fe_2C_{74}H_{76}N_{10}Cl_2O_{14}$: C, 58.78; H, 5.07; N, 9.26%. Molar conductivity (S mol^{-1} cm^2) 291. IR (KBr) ν_{as}(COO) 1555, ν_s(COO) 1435 cm^{-1}.

[Fe$_2$(Me$_4$-tpdp)(C$_6$H$_5$CO$_2$)(H$_2$O)](BF$_4$)$_2$ (5) and [Fe$_2$(Me$_4$-tpdp)(CF$_3$CO$_2$)(H$_2$O)$_2$](BF$_4$)$_2$·H$_2$O (6). The complexes were prepared as described elsewhere.[9b]

[Co$_2$(tpdp)(CH$_3$CO$_2$)](ClO$_4$)$_2$ (7). The complex was prepared as described previously.[14d]

[Co$_2$(bpmp)(C$_6$F$_5$CO$_2$)](ClO$_4$)$_2$ (8). The complex was prepared in a similar way to that of $[Co_2(bpmp)(C_6H_5CO_2)](ClO_4)_2$.[14c] To a solution of Hbpmp (133 mg, 0.25 mmol), $Co(ClO_4)_2{\cdot}6H_2O$ (183 mg, 0.5 mmol), and $C_6F_5CO_2H$ (53 mg, 0.25 mmol) in 15 cm^3 of methanol was added a solution of triethylamine (25 mg, 0.25 mmol) in 5 cm^3 of methanol with stirring. The resulting solution was allowed to stand overnight to give orange crystals. Found: C, 45.72; H, 2.98; N, 7.83%. Calcd for $Co_2C_{40}H_{33}N_6Cl_2F_5O_{11}$: C, 45.43; H, 3.15; N, 7.95%. IR ν_{as}(COO) 1657m, ν_s(COO) 1387 cm^{-1}.

[Co$_2$(bpmp)(CF$_3$CO$_2$)](ClO$_4$)$_2$ (9). To a solution of Hbpmp (133 mg, 0.25 mmol) and $Co(ClO_4)_2{\cdot}6H_2O$ (183 mg, 0.5 mmol) in 10 cm^3 of ethanol was added a solution of CF_3CO_2Na (34 mg, 0.25 mmol) in 5 cm^3 of ethanol with stirring. The resulting solution was allowed to stand overnight to give orange crystals. Found: C, 43.91; H, 3.35; N, 8.66%. Calcd for $Co_2C_{35}H_{33}N_6Cl_2F_3O_{11}$: C, 43.82; H, 3.47; N, 8.76%. IR ν_{as}(COO) 1695, ν_s(COO) 1442 cm^{-1}.

[Co$_2$(Me$_4$-tpdp)(CH$_3$CO$_2$)](ClO$_4$)$_2$·2H$_2$O (10). To a solution of Me$_4$-Htpdp (255 mg, 0.5 mmol) and $Co(CH_3CO_2)_2{\cdot}4H_2O$ (246 mg, 1.0 mmol) in 10 cm^3 of methanol was added a solution of $NaClO_4{\cdot}H_2O$ (425 mg, 3.0 mmol) in 5 cm^3 of methanol with stirring. The resulting solution was allowed to stand overnight to give violet crystals. Found: C, 42.59; H, 4.51; N, 9.23%. Calcd for $Co_2C_{33}H_{44}N_6Cl_2O_{13}$: C, 43.01; H, 4.81; N, 9.12%. IR ν_{as}(COO) 1573, ν_s(COO) 1443 cm^{-1}.

[Co$_2$(bpmp)(C$_6$F$_5$CO$_2$)$_2$]ClO$_4$ (11). The complex was prepared in a similar way to that of $[Co_2(bpmp)(C_6H_5CO_2)_2]ClO_4$.[14c] To a solution of $Co(ClO_4)_2{\cdot}6H_2O$ (183 mg, 0.5 mmol) in 5 cm^3 of methanol was added a mixture of Hbpmp (133 mg, 0.25 mmol), $C_6F_5CO_2H$ (106 mg, 0.5 mmol) and triethylamine (75 mg, 0.75 mmol) in 10 cm^3 of methanol. The resulting solution was allowed to stand overnight to give red crystals, which were collected by filtration, washed with methanol and ether, and dried in vacuo. Found: C, 48.31; H, 2.58; N, 7.23%. Calcd for $Co_2C_{47}H_{33}ClF_{10}N_6O_9$: C, 48.29; H, 2.85; N, 7.19%. IR ν_{as}(COO) 1657, ν_s(COO) 1381 cm^{-1}.

[Co$_2$(bpmp)(CF$_3$CO$_2$)$_2$]BPh$_4$·CH$_3$COCH$_3$ (12). The complex was prepared in the same way as that for **11**, except that CF_3CO_2H was used instead of $C_6F_5CO_2H$. Addition of $NaBPh_4$ afforded red crystals. Found: C, 61.45; H, 4.75; N, 6.72%. Calcd for $Co_2C_{64}H_{59}BF_6N_6O_6$: C, 61.95; H, 4.57; N, 6.76%. IR ν_{as}(COO) 1701, ν_s(COO) 1446 cm^{-1}.

Measurements. Electronic spectra were measured on a Hitachi U-3400 spectrophotometer equipped with an Otsuka Denshi optical glass fiber attachment and an Otsuka Denshi MCPD 2000 spectrophotometer. Infrared spectra were obtained by the KBr-disk method with a Horiba FT-200 spectrophotometer. Cyclic voltammograms were measured with a Hokuto Denko HA-301 Potentiostat/Galvanostat and a Hokuto Denko HB-104 Function Generator by using a three-electrode configuration, including a glassy carbon working electrode, a platinum-coil auxiliary electrode, and a saturated calomel electrode as a reference electrode. Acetonitrile and CH_2Cl_2 were used as the solvent, and tetrabutylammonium perchlorate as a supporting electrolyte. The $E_{1/2}$ values of ferricinium/ferrocene (Fc^+/Fc) in acetonitrile and CH_2Cl_2 were 395 mV and 540 mV vs. SCE, respectively, with this setup. Molar conductivities were measured at 25 °C in acetonitrile (1×10^{-3}

mol dm^{-3}) with a Toa CM-20S conductivity meter. ^{1}H NMR spectra were measured with a JEOL GX 400 spectrometer by using tetramethylsilane (TMS) as the internal reference standard. Spectra were collected over a 160 kHz bandwidth with 16000 data points and an 8 μs 90° pulse. For a typical spectrum, 1000 to 4000 transients were accumulated with a 30-ms pulse delay time.

Dioxygen Affinity Measurement. The equilibrium constant (K) of Eq. 1 for the oxygenation reaction was determined by spectrophotometric titration in acetonitrile or CH_2Cl_2 at various temperatures.

$$M_2 + O_2 \overset{K}{\rightleftharpoons} M_2(O_2) \quad (1)$$
$$K = \frac{[M_2(O_2)]}{[M_2]P(O_2)}$$

The reaction temperatures were controlled with an Advantec Lab Thermo Cool LCH-4V above 10 °C and a Tokyo Rikakikai Eyela Low Temp. Pair Stirrer PSL-80 and a Neslab Cryobath CB-80 with a Cryotrol temperature controller for low temperatures. Experimental details were given elsewhere.[9b]

The equilibrium constant (K) was calculated by the following equation: $P(O_2) = C{\cdot}P(O_2)/\Delta A - K^{-1}$, where $P(O_2)$ is the partial pressure of O_2, ΔA is the difference between the absorbances of the solution at $P(O_2)$ and $P(O_2) = 0$ Torr, and C is a constant.[17] Plots of $P(O_2)$ vs. $P(O_2)/\Delta A$ for all the complexes gave a straight line, indicating a 1 : 1 (complex: O_2) stoichiometry for the oxygenation.

O_2 Uptake Measurement. Gas uptake measurements were carried out in a similar way to that described in the literature except that an ampule (ca. 3 cm^3) was used as a sample container instead of a sample reservoir.[18] The system consists of a three-necked reaction flask (100 cm^3), an ampule containing the complex, and a gas burette (20 cm^3), which is given in the supplementary materials.[19] A weighed amount of the complex (ca. 0.5 mmol) was placed inside an ampule, and the ampule was connected to a vacuum line to evacuate it; the ampule was sealed after evacuation. Before use, the volumes of the ampules were estimated by pouring water into them and weighing the water contained. The volumes of the ampules were calibrated without complex by breaking the ampules. The differences between the estimated volumes and the measured ones were within ±0.2 cm^3. The ampule was suspended into the reaction flask. The reaction flask was charged with CH_2Cl_2 under O_2 atmosphere and immersed at a low temperature. After the system was equilibrated, the ampule was broken. The gas uptakes were completed within 1 h. The uptakes of O_2 by **1** and **2** are 1 : 0.95±0.05 (complex: O_2).

X-Ray Crystallography. [Fe$_2$(Ph-tidp)(C$_6$H$_5$CO$_2$)](ClO$_4$)$_2$·2CH$_3$CN·(C$_2$H$_5$)$_2$O·H$_2$O (1). A single crystal of **1** was obtained by a slow diffusion of diethyl ether into an acetonitrile solution. Since crystals were very efflorescent at room temperature, a single crystal was picked up on a hand-made cold copper plate mounted inside a liquid N_2 Dewar vessel and mounted on a glass rod at −80 °C. Data were collected at −120 °C on a Rigaku RAXIS-IV imaging plate area detector using graphite monochromated Mo $K\alpha$ radiation (λ = 0.71070 Å). Crystal-to-detector distance was 120 mm. In order to determine the cell constants and the orientation matrix, three oscillation photographs were taken with oscillation angle 2° and exposure time of 8 min for each frame. Intensity data were collected by taking oscillation photographs (total oscillation range 120°; 80 frames; oscillation angle 1.5°; exposure time 14 min). The data were corrected for Lorentz and polarization effects, but not for absorption effect.

The unit-cell parameters used for the refinement were determined by least-squares calculations on the setting angles for 25 reflections with $22.69° < 2\theta < 23.63°$ that were collected on a Rigaku AFC-7R four circle automated diffractometer. Crystallographic data are summarized in Table 1.

The structure was solved by a direct method (SHELX-86)[20] and expanded using a Fourier technique.[21] All non-hydrogen atoms were refined by full-matrix least-squares methods with anisotropic displacement parameters. Hydrogen atoms were included but not refined. The final values of the agreement factors were $R = 0.060$, $R_w = 0.084$. A final difference Fourier map showed the largest peaks of 0.78 and −0.77 e Å^{-3}. Experimental details for X-ray crystallography, tables of final atomic coordinates, thermal parameters, full bond distances and angles, and lists of F_o and F_c are given in the supplementary materials.[19]

Results

Characterization of Complexes. All the Ph-tidp complexes form monocarboxylato complexes, [Fe$_2$(Ph-tidp)(RCO$_2$)]$^{2+}$, in which both the metal centers are five-coordinate (vide infra). The Ph-tidp complexes are air-stable in solid state except for **4**, but react with dioxygen in CH_2Cl_2 and CH_3CN. Reactivity of those complexes in solution state is highly dependent on the temperature. At room temperature, the complexes gradually oxidized irreversibly to give a brown solution, whereas below −20 °C the complexes reacted rapidly with dioxygen to show deep dark-green color of oxygenated-species (vide infra). Dioxygen consumptions of **1** and **2** at −75 °C are 1 : 0.95±0.05 (complex : O_2), indicating the formation of peroxo species as found for the Me$_4$-tpdp[9b] and Ph-bimp[10] complexes.

X-Ray Structure Description of 1. The molecular structure of the dinuclear cation of **1** is shown in Fig. 1.

Table 1. Crystallographic Data for [Fe$_2$(Ph-tidp)(C$_6$H$_5$CO$_2$)](ClO$_4$)$_2$·2CH$_3$CN·(C$_2$H$_5$)$_2$O·H$_2$O (**1**)

Formura	$Fe_2C_{86}H_{88}O_{13}N_{12}Cl_2$
Fw	1680.31
Space group	$P2_1/c$
a/Å	13.464(2)
b/Å	19.223(4)
c/Å	31.358(4)
β/deg	92.84(2)
V/Å^3	8106(2)
Z	4
Crystal size/mm	0.25×0.10×0.05
ρ_{calcd}/g cm^{-3}	1.377
λ(Mo $K\alpha$)/Å	0.71070
Oscillation range/deg	120.00
Oscillation angle per frame/deg	1.5
Maximum 2θ value/deg	51.6
No. of data collected	13283
No. of data used ($>3\sigma(I)$)	8881
No. of variables	970
Temperature/°C	−120
μ/cm^{-1}	4.95
F(000)	3512.00
R	0.060
R_w	0.084
Goodness of fitness	1.36

The selected bond distances and angles are given in Table 2. Two iron centers are five-coordinate with N_3O_2 donor set and doubly bridged by the alkoxide oxygen of Ph-tidp and the benzoate oxygens as found for a closely related complex, $[Fe_2(NEt\text{-}HPTB)(C_6H_5CO_2)](BF_4)_2$ (**15**), reported by Que et al.,[8a] which has 2-benzimidazolyl groups as side arms. The structures of two five-coordinate iron centers differ from each other; one has a distorted trigonal bipyramidal structure, whereas the other has a distorted square-pyramidal structure. The average Fe–N(imidazole) bond distance of **1** is 2.12 Å, which is substantially longer than the average Fe–N(benzimidazolyl) bond distance of **15** (2.07 Å). The elongation of the Fe–N(imidazolyl) in **1** compared to that of

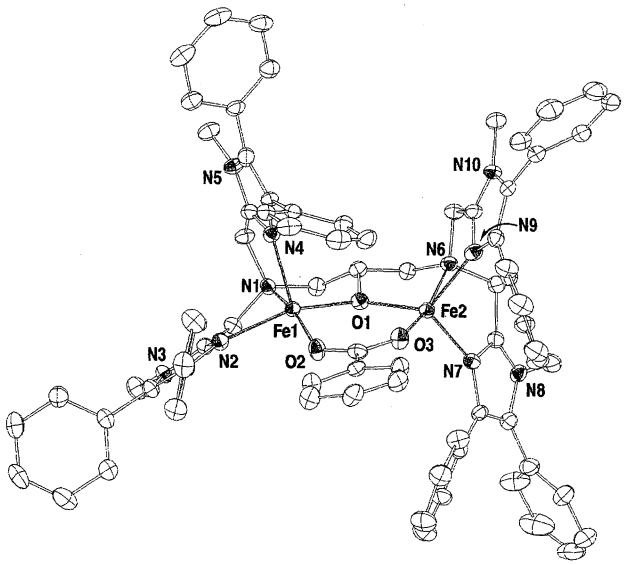

Fig. 1. ORTEP view of a complex cation $[Fe_2(Ph\text{-}tidp)(C_6H_5CO_2)]^{2+}$ (**1**).
The non-hydrogen atoms are represented by 50% probability thermal ellipsoids. The hydrogen atoms are omitted for clarity.

Table 2. Selected Bond Lengths and Bond Angles of **1**

	Bond lengths (Å) (**1**)		
Fe1···Fe2	3.592(1)		
Fe1–O1	2.003(4)	Fe2–O1	2.004(4)
Fe1–O2	2.000(4)	Fe2–O3	2.006(4)
Fe1–N1	2.365(4)	Fe2–N6	2.268(4)
Fe1–N2	2.131(4)	Fe2–N7	2.131(4)
Fe1–N4	2.092(4)	Fe2–N9	2.142(4)
	Bond angles (deg) (**1**)		
O1–Fe1–O2	95.8(1)	O1–Fe2–O3	95.1(1)
O1–Fe1–N1	80.0(1)	O1–Fe2–N6	80.0(1)
O1–Fe1–N2	145.2(1)	O1–Fe2–N7	111.0(1)
O1–Fe1–N4	100.3(2)	O1–Fe2–N9	126.5(2)
O2–Fe1–N1	161.4(1)	O3–Fe2–N6	167.9(2)
O2–Fe1–N2	98.2(2)	O3–Fe2–N7	114.4(2)
O2–Fe1–N4	122.1(2)	O3–Fe2–N9	99.0(2)
N1–Fe1–N2	76.6(1)	N6–Fe2–N7	77.7(2)
N1–Fe1–N4	76.5(1)	N6–Fe2–N9	75.6(2)
N2–Fe1–N4	98.9(2)	N7–Fe2–N9	109.1(2)

15 seems to be partly due to unfavorable steric interactions between 4-phenyl substituents of 2-imidazolyl groups and the bridging benzoate which resides in a cavity formed by four 4-phenyl substituents of 2-imidazolyl groups. A similar observation was made for **5**, which has sterically bulky 6-methyl substituent of 2-pyridyl group.[9b] Elongation of the Fe–N bond distance due to introduction of phenyl substituents into 2-imidazolyl group also becomes clear by comparison of the Fe–N bond distances in the mixed valence high-spin diiron(II, III) complexes, $[Fe_2(Ph\text{-}bimp)(C_6H_5CO_2)_2]^{2+}$ (**16**) ($Fe\text{–}N_{av}$(imidazolyl) = 2.18 and 2.20 Å for iron(III) and iron(II) centers, respectively)[22] and $[Fe_2(bimp)(C_6H_5CO_2)_2]^{2+}$ (**17**) ($Fe\text{–}N_{av}$(imidazolyl) = 2.10 and 2.12 Å for iron(III) and iron(II) centers, respectively).[23] It should be noted that the average Fe–N(pyridyl) bond distance of a five-coordinate iron center in **5** is 2.19 Å, which is significantly longer than that in **1**. Such a remarkable elongation of the Fe–N bonds in **5** compared to that in **1** implies that steric influence of 6-methyl-2-pyridyl group is greater than that of 4,5-diphenyl-2-imidazolyl group in these complexes.

Electronic Spectra. It is well known that the d–d transition of high-spin iron(II) complexes is useful to determine the stereochemistry around the iron(II) center; six-coordinate complexes show two d–d bands with a splitting of 1000—2000 cm^{-1} at about 10000 cm^{-1} which are splitting components of the electronic transitions from $^5T_{2g}$ to ^5E_g (in octahedral symmetry), while for five-coordinate complexes, the splitting is much larger than that of six-coordinate complexes and their electronic spectra display two d–d bands near 10000 cm^{-1} and near 5000 cm^{-1}.[24] All the Ph-tidp iron complexes showed two d–d bands at 5000—6000 cm^{-1} and 11000—12000 cm^{-1} both in solution and solid states, indicating that iron centers are five-coordinate (Fig. 2 and Table 3). The Me_4-tpdp iron complexes have been shown to take five-coordinate structure in CH_2Cl_2.[9b] It was found that **5**[9b] and **15**[8b] reacted with DMSO to form a six-coordinate species, whereas **1** did not form a six-coordinate species even in DMSO. 4,5-Diphenyl-2-imidazolyl group tends to stabilize a five-coordinate structure compared to 6-methyl-2-pyridyl and 2-benzimidazolyl groups. This is probably due to steric bulkiness of substituents in dinucleating ligands and Lewis acidity of iron centers. The electron donor ability of 6-methyl-2-pyridyl group is weaker than that of 4,5-diphenyl-2-imidazolyl group, which is clearly seen from electrochemistry (vide infra). This will lead to a higher Lewis acidity of iron center in **5** compared to that in **1**. Higher Lewis acidity of iron center would favor a six-coordinate structure. This is probably the case for **5**. On the other hand, the electron donor ability of 2-benzimidazolyl group is expected to be comparable to that of 4,5-diphenyl-2-imidazolyl group by comparison of $E_{1/2}$ value of a mixed valence diiron(II, III) complex, $[Fe_2(bzimp)(C_6H_5CO_2)_2]^{2+}$ (**18**) ($E_{1/2} = -30$ mV vs. SCE for Fe(II, III)/Fe(II, II) couple)[25] which contains 2-benzimidazolyl side arms with that of **16** ($E_{1/2} = -30$ mV vs. SCE for Fe(II, III)/Fe(II, II) couple).[22] Formation of a six-coordinate species of **15** by addition of DMSO suggests that steric bulkiness of 2-benzimidazolyl group is not enough to

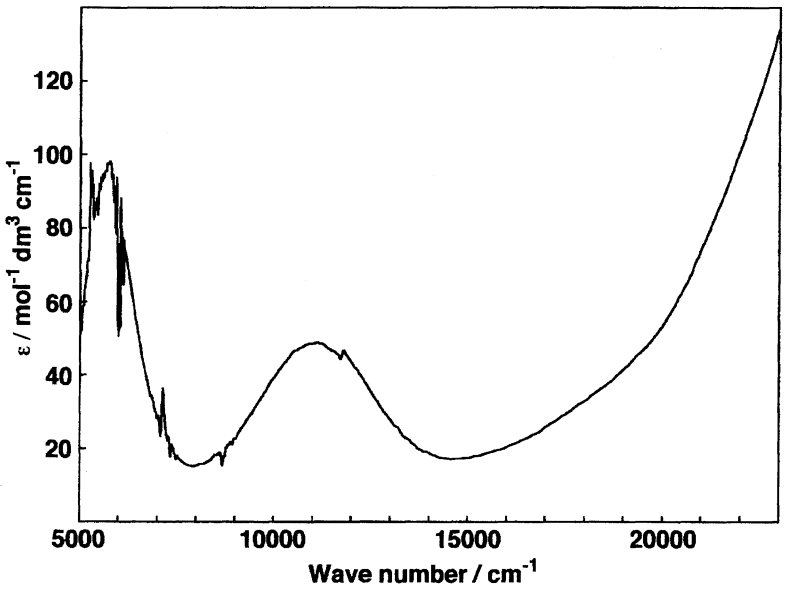

Fig. 2. Electronic spectrum of **1** in CH_2Cl_2.

Table 3. Electronic Spectral Data of Diiron(II) Complexes in CH_2Cl_2 and Dicobalt(II) Complexes in CH_3CN

Complexes	Band maxima			
	$\tilde{\nu}$/cm^{-1} (ε/mol^{-1} dm^3 cm^{-1})			
1	11140 (50)	ca. 5780 (ca. 100)		
in DMSO	10920 (30)	ca. 5780 (ca. 50)		
Reflectance	ca. 12000	ca. 5780		
2	11110 (54)	ca. 5850 (ca. 73)		
3	10870 (31)	ca. 5880 (ca. 73)		
Reflectance	ca. 10800	ca. 5850		
4	10870 (50)	ca. 5710 (ca. 72)		
5[a]	11850 (30)	ca. 5800 (ca. 70)		
Reflectance	ca. 12400	ca. 8000b	ca. 6000	
6[a]	11980 (18)	ca. 6100 (ca. 35)		
Reflectance	ca. 12000	ca. 8000		
8	6500[b] (13)	10290[b] (18)	15500[c] (40)	18120[c] (133)
9	6500[b] (9)	9790[b] (17)	15500[c] (30)	18000[c] (95)
11	9560 (19)	20580 (48)		
12	9770 (22)	22030 (121)		

a) Ref. 9b. b) Broad band. c) Shoulder.

prevent formation of a six-coordinate species.

The electronic spectra of **8** and **9** in acetonitrile show several d–d bands in the visible and near infrared regions (Table 3), characteristic of those of the five-coordinate cobalt(II) complexes which have been shown to exhibit several d–d bands in the 5000—25000 cm^{-1} region.[26] In contrast, the corresponding bis(carboxylato) complexes, **11** and **12** which have six-coordinate structure, showed only two d–d bands at ca. 10000 and 20000—22000 cm^{-1}.

Electrochemistry. Cyclic voltammograms (CV) of all the diiron complexes, **1**—**6** in CH_2Cl_2 showed two quasi-reversible waves, which correspond to Fe_2(II, III)/Fe_2(II, II) and Fe_2(III, III)/Fe_2(II, III) redox couples (Table 4). CV of **1** is exemplified in the supplementary materials.[19] $E_{1/2}$ values of the Ph-tidp complexes are dependent on the bridging carboxylates ($C_2H_5CO_2 < C_6H_5CO_2 < C_6F_5CO_2 < CF_3CO_2$) which are well correlated with the electron donor ability of the bridging carboxylates. As the electron donor becomes weaker, $E_{1/2}$ value becomes positive. $E_{1/2}$ values of **5** and **6** are 605 and 750 mV vs. SCE, respectively, which are significantly positive compared to those of the corresponding Ph-tidp complexes. This positive shift of $E_{1/2}$ values for the Me_4-tpdp complexes is partly ascribed to weaker electron donor ability of the 6-methyl-2-pyridyl group compared to that of 4,5-diphenyl-2-imidazole group, which is in line with the observation that elongation of the Fe–N bond distances in **5** is remarkable compared to that in **1**.

Oxygenation Reaction. All the Ph-tidp complexes reacted reversibly with dioxygen to show intense dark-green color in CH_2Cl_2 and CH_3CN below -20 °C, which can be attributable to CT transition from the peroxo π^* orbital to iron(III) d orbitals, characteristic of μ-peroxo diiron species. The

Table 4. CV Data of Diiron(II) Complexes in CH_2Cl_2

Complex	$E_{1/2}$(II, III/II, II)	$E_{1/2}$(III, III/II, III)
	mV vs. SCE	mV vs. SCE
1	460 (310)	950 (180)
2	505 (240)	970 (210)
3	605 (320)	1080 (310)
4	445 (230)	955 (190)
5[a]	605	995
6[a]	750	1260
16[b]	−30[d] (110)	640 (120)
17[c]	−180[d,e]	477

a) Ref. 9b. b) Ref. 22. c) Ref. 23. d) Measured in CH_3CN. e) Values reported vs. AgCl/Ag.

electronic spectral data are given in Table 5. Warming the intense dark-green solution up to room temperature restored the original pale yellow color even under O_2 atmosphere, while the corresponding Me_4-tpdp complexes underwent irreversible oxidation in the same conditions. Electronic spectral change of this process for **1** is exemplified in Fig. 3. Regeneration of the diiron(II) species was clearly confirmed from the electronic spectra (c) in Fig. 3 which is almost identical to the original one (a). The same observation was made in NMR spectral change. Reasonable reversibility was observed for all the complexes **1**—**4**. Dioxygen consumptions of **1** and **2** upon exposure to O_2 at −75 °C are 1 : 0.95±0.05 (complex : O_2), also supporting the formation of oxygenated-species as found for the Me_4-tpdp and Ph-bimp complexes. Although we tried to measure the resonance Raman spectra of dark-green species to confirm the formation of peroxo species at −40 °C, all the measurements were in vain so far, probably due to photolability of the peroxo-species.

The dioxygen-iron complexes have been shown to be highly susceptible to irreversible oxidation. In the previous studies, we demonstrated that sterically bulky substituents of the present type of dinucleating ligands which weaken the electron donor ability and form a hydrophobic cavity for a O_2 binding site can suppress the irreversible oxidation and facilitate the reversible oxygenation. Comparison of the thermal stability of the oxygenated-Ph-tidp species with that of the oxygenated-Me_4-tpdp and oxygenated-Ph-bimp species is very interesting. Irreversible oxidation can be monitored spectrophotometrically; an intense dark-green color of oxygenated-species faded upon irreversible oxidation. Preliminary measurement indicates that decay of oxygenated-**1**, -**3**, -**4**, -**5**, and -**6** in CH_2Cl_2 follows the first order rate law under 1 atom of O_2, similar to that found for **15**.[11] Their half life times ($t_{1/2}$) under 1 atom of O_2 at −40 °C are also given in Table 5. The data suggest that the oxygenated-Ph-tidp complexes are thermally more stable than the corresponding oxygenated-Me_4-tpdp species. Below −60 °C, no measurable decay was observed for all the oxygenated-Ph-tidp complexes. Thus introduction of 4,5-diphenyl substituents into 2-imidazolyl group also stabilizes thermal stability of oxygenated-species as well as 6-methyl substituent of 2-pyridyl group. Reversibility of the oxygenation is improved for the Ph-tidp complexes as compared with the Me_4-tpdp complexes.

Dicobalt complexes **8** and **9** also reacted reversibly with dioxygen to show intense brown color in CH_2Cl_2 and CH_3CN at room temperature, as found for $[Co_2(bpmp)(C_6H_5CO_2)(O_2)]^{2+}$.[14a—14c] The electronic spectral data are also given in Table 5. The intense absorption at 21500—26000 cm^{-1} can be assigned to CT transition from the peroxo π^* orbital to cobalt(III) d_σ^* orbitals, characteristic of the μ-peroxo dicobalt

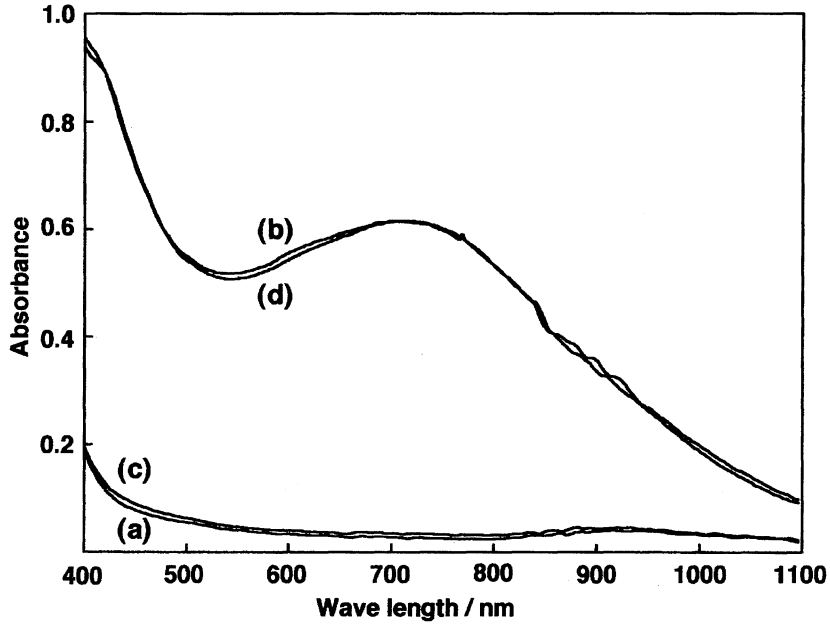

Fig. 3. Electronic spectral change of **1** in CH_2Cl_2 under O_2.
The spectra of (a)—(d) show the repetition of reversible oxygenation–deoxygenation cycles; (a) and (c) were measured at room temperature, and (b) and (d) at −60 °C, respectively.

Table 5. Electronic Spectral Data of Oxygenated Diiron Species in CH_2Cl_2 at −40 °C and Oxygenated Dicobalt Species in CH_3CN at 20 °C and Half-Life Time ($t_{1/2}$) of Oxygenated Diiron Species under 1 atm of O_2

Complexes	Band maxima $\tilde{\nu}$/cm^{-1} (ε/mol^{-1} dm^3 cm^{-1})	$t_{1/2}$ (°C)	
Oxy-**1**	13930 (2000)	8.6 h	(−20 °C)
		30 h	(−31 °C)
		52 h	(−42 °C)
		a)	(−60 °C)
in CH_2Cl_2/DMF (4 : 1 v/v)	14250 (1800)		
in CH_2Cl_2/DMSO (4 : 1 v/v)	14450 (1600)		
Oxy-**2**	14810 (2200)	a)	(−60 °C)
Oxy-**3**	15110 (2700)	50 h	(−40 °C)
		a)	(−70 °C)
Oxy-**4**	14120 (2000)	139 h	(−41 °C)
Oxy-**5**	16530 (2200)	24 h	(−40 °C)
Oxy-**6**	16310 (4000)	31 h	(−40 °C)
Oxy-**14**[b)]	12500—20000 (1700)		
Oxy-**15**[c)]	17000 (1500)		
Oxy-**13**[d)]	14730 (3450)		
Oxy-Hr[e)]	20000 (2300)		
Oxy-**7**[f)]	25640 (4500)		
Oxy-**8**	21550 (3020)		
Oxy-**9**	21550 (2420)		

a) At least several days. b) Ref. 10 c) Ref. 8b d) Ref. 7b e) Ref. 27 f) Ref. 14d.

complexes.[28)] Complex **7** did not react with dioxygen at room temperature, but reacted below 0 °C.[14d)] This suggests that dioxygen affinity of this complex is very low. Reversibility of all dicobalt complexes are fairly good and no measurable irreversible oxidation was observed after several cycles of oxygenation-deoxygenation.

Dioxygen Affinity. Since all the complexes showed reasonable reversible oxygenation, dioxygen affinities of diiron(II) and dicobalt(II) complexes were measured at various temperatures. As mentioned in the experimental section, plots of $P(O_2)$ vs. $P(O_2)/\Delta A$ for all the complexes gave straight lines, indicating a 1 : 1 (complex : O_2) stoichiometry for the oxygenation (Figs. 4, 5, and 6). Enthalpy and entropy changes were estimated from van't Hoff plots (Fig. 7). Thermodynamic data are given in Table 6 together with $P_{1/2}$ values, which correspond to $1/K$. Since the temperature range of the oxygenation of the present complexes is wide, comparison of dioxygen affinities of complexes is made in terms of $P_{1/2}$ values extrapolated at 20 °C. Although those values, especially for the complexes which react with dioxygen at low temperature, are only rough measures because of the large errors in enthalpy and entropy, those are convenient for qualitative comparison of dioxygen affinities. The changes in the dinucleating ligand and the bridging carboxylate have a pronounced influence on the dioxygen affinity.

Discussion

In the previous studies, we found that sterically bulky ligands are effective to prevent the irreversible oxidation of μ-peroxo diiron species. Ph-tidp also tends to stabilize μ-peroxo diiron species. These findings suggest that the introduction of a sterically bulky substituent into the 2-pyridyl or 2-imidazolyl group of the dinucleating ligands suppresses some deleterious, irreversible decay reactions of μ-peroxo species, as mentioned before.[9b,10)] If the decay reaction proceeds via a higher valent species such as Fe(IV), a weaker electron donor appears to be effective to prevent the formation of an Fe(IV) species and to facilitate the regeneration of diferrous species from μ-peroxo diferric species. If the decay reaction is bimolecular, the steric properties of the ligand also seem to be important, because the sterically bulkier ligand which can form a hydrophobic cavity surrounding the O_2-binding site would provide unfavorable interactions in the transition state of the decay reaction. In either case, a sterically bulky substituent would suppress the irreversible oxidation and facilitate the reversible oxygenation. Thus weaker electron donor and sterically bulkier ligand play an important role for controlling thermal stability of μ-peroxo diiron species.

It is well known that dioxygen affinity of the cobalt complexes which have a quite similar structure is dependent on the electron donor ability of ligand; the stronger the electron donor ability of the ligand, the greater the electron density on cobalt center, the easier the electron drift from cobalt to dioxygen, and the higher the dioxygen affinity.[29,30)] The electrochemistry of the Ph-tidp complexes shows that the order of the electron donor ability of the bridging carboxylates is $C_2H_5CO_2 > C_6H_5CO_2 > C_6F_5CO_2 > CF_3CO_2$. Within the Ph-tidp complexes (**1**, **2**, and **3**), dioxygen affinity is well correlated with the electron donor ability of the bridging ligands, although the ΔH and ΔS variations in these complexes are random.

Comparison of the dioxygen affinity of the Me_4-tpdp and Ph-tidp complexes is interesting. The electron donor abil-

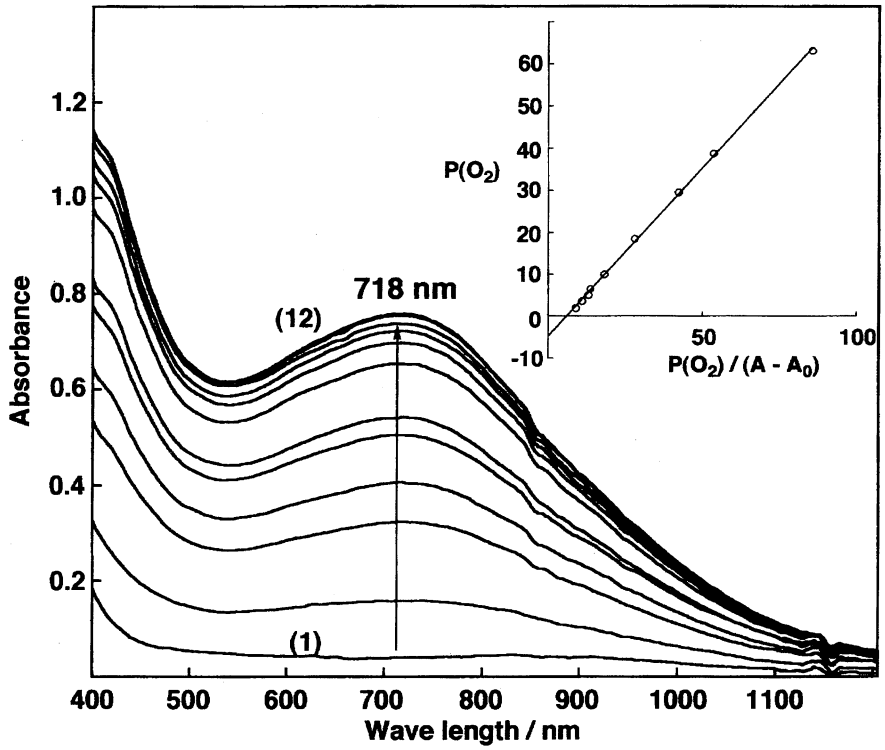

Fig. 4. Spectral change of **1** at various dioxygen partial pressures in CH_2Cl_2 at −54 °C: (1) 0 Torr, (2) 1.9 Torr, (3) 3.6 Torr, (4) 5.0 Torr, (5) 6.4 Torr, (6) 9.9 Torr, (7) 18 Torr, (8) 30 Torr, (9) 39 Torr, (10) 63 Torr, (11) 89 Torr, (12) 120 Torr. Insert is a plot of $P(O_2)$ vs. $P(O_2)/\Delta A$. Data obtained from spectra (11) and (12) are omitted from $P(O_2)$ vs. $P(O_2)/\Delta A$ plot because almost saturation occurred at these dioxygen partial pressures. See in text.

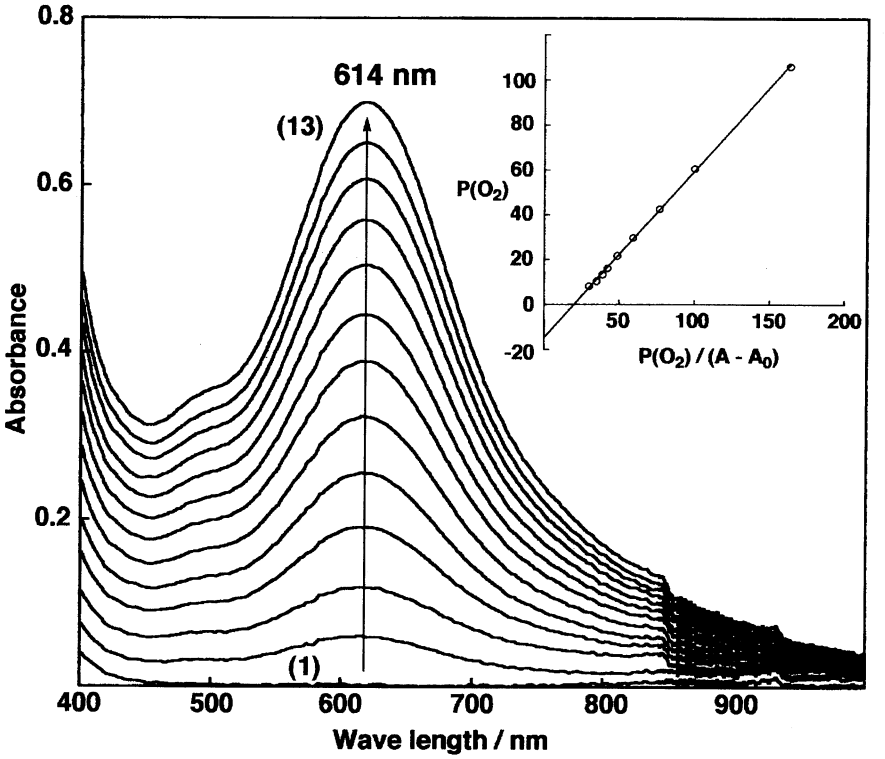

Fig. 5. Spectral change of **6** at various dioxygen partial pressures in CH_2Cl_2 at −51 °C: (1) 0 Torr, (2) 3.3 Torr, (3) 4.8 Torr, (4) 8.2 Torr, (5) 10 Torr, (6) 13 Torr, (7) 16 Torr, (8) 22 Torr, (9) 30 Torr, (10) 43 Torr, (11) 615 Torr, (12) 106 Torr, (13) 286 Torr. Insert is a plot of $P(O_2)$ vs. $P(O_2)/\Delta A$. Data obtained from spectra (2) and (3) are omitted from $P(O_2)$ vs. $P(O_2)/\Delta A$ plot because of poor reproducibility due to very slow oxygenation equilibrium at low dioxygen partial pressure. See in text.

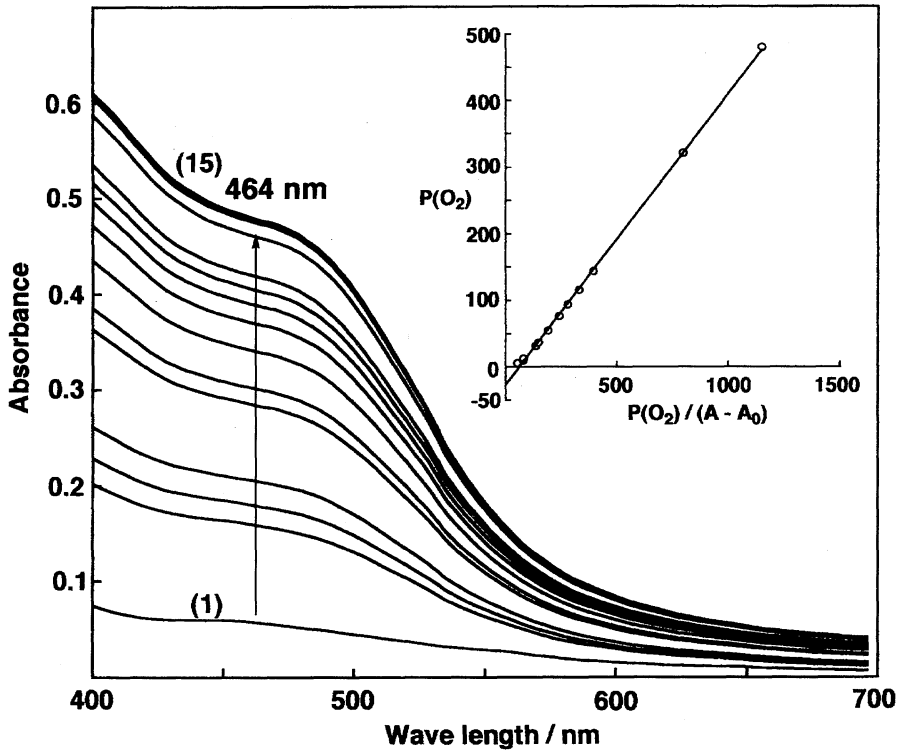

Fig. 6. Spectral change of **9** at various partial dioxygen pressures in CH_3CN at 20 °C: (1) 0 Torr, (2) 5.5 Torr, (3) 10 Torr, (4) 12 Torr, (5) 31 Torr, (6) 36 Torr, (7) 54 Torr, (8) 76 Torr, (9) 93 Torr, (10) 115 Torr, (11) 143 Torr, (12) 321 Torr, (13) 480 Torr, (14) 524 Torr, (15) 563 Torr.
Insert is a plot of $P(O_2)$ vs. $P(O_2)/\Delta A$. Data obtained from spectra (14) and (15) are omitted from $P(O_2)$ vs. $P(O_2)/\Delta A$ plot because saturation occurred at these dioxygen partial pressures. See in text.

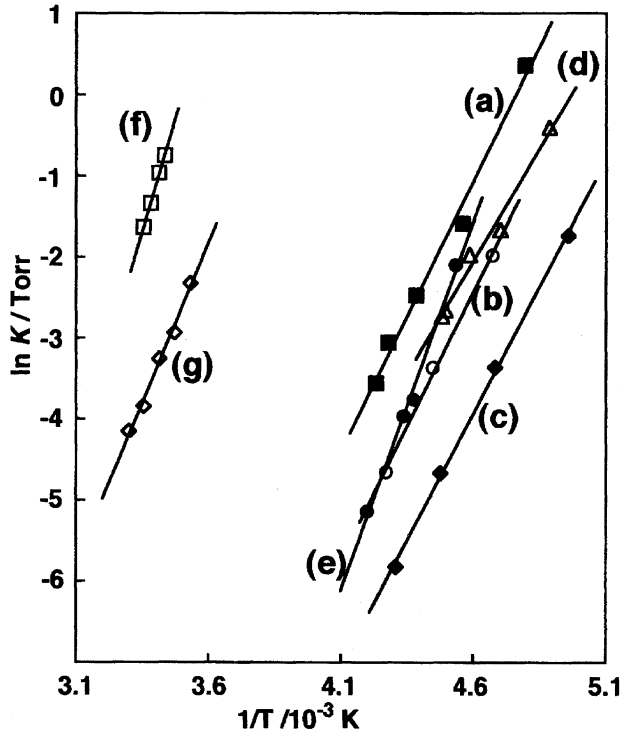

Fig. 7. van't Hoff plots for oxygenation of complexes: (a) **1**, (b) **2**, (c) **3**, (d) **6**, (e) **7**, (f) **8**, (g) **9**.

ity of Me_4-tpdp is weaker than that of Ph-tidp. Dioxygen affinity of **6**, however, is greater than those of the Ph-tidp complexes. This is in contrast to the observation for the Ph-tidp complexes with different bridging carboxylates. The enthalpy change for **6** (-47 kJ mol^{-1}) is more positive (less favorable) than those for the Ph-tidp complexes (-52——-55 kJ mol^{-1}), whereas the entropy change for **6** (-231 J mol^{-1} K^{-1}) is less negative (more favorable) than those for the Ph-tidp complexes (-263——-274 J mol^{-1} K^{-1}). Favorable entropy change for **6** overcomes less favorable enthalpy change, leading to higher dioxygen affinity compared to those of the Ph-tidp complexes.

Reactivity of iron complexes with dioxygen is much higher than that of the corresponding cobalt complexes with the same ligand system. For example, **5** reacts with O_2 to form an oxygenated-species at -40 °C, whereas the corresponding cobalt(II) complex, $[Co_2(Me_4\text{-tpdp})(CH_3CO_2)]^{2+}$ (**10**), has no reactivity with O_2, suggesting that electron density on cobalt(II) ion in **10** seems to be not enough to transfer electrons to O_2 to produce O_2^{2-}. In fact, cyclic voltammogram of **10** showed that electrochemical oxidation does not occur until +1.2 V vs. SCE, suggesting that **10** is not much oxidized by O_2. Thus a stronger electron donor is necessary for oxygenation of cobalt complexes compared to that of iron complexes. In contrast, complex **7**, which has no methyl substituent on 2-pyridyl group, reacts with O_2 below 0 °C to form an oxygenated-species in CH_2Cl_2. Thus introduction of 6-methyl substituent into 2-pyridyl group also has a sig-

Table 6. Thermodynamic Data for Oxygenation of Diiron(II) and Dicobalt(II) Complexes

Complex	$P_{1/2}$/Torr at 20 °C[b]	ΔH/kJ mol^{-1} ΔS/J mol^{-1} K^{-1}	T/K	$K(O_2)$/Torr^{-1} [a]
1	8600	−55±3 (ΔH)	208	1.4
		−263±14 (ΔS)	219	2.1×10^{-1}
			228	8.4×10^{-2}
			233	4.7×10^{-2}
			236	2.8×10^{-2}
in CH_2Cl_2/DMF (4 : 1 v/v)			233	4.2×10^{-2}
in CH_2Cl_2/DMSO (4 : 1 v/v)			232	2.5×10^{-2}
2	32000	−55±3 (ΔH)	214	1.4×10^{-1}
		−274±12 (ΔS)	225	3.4×10^{-2}
			234	9.5×10^{-3}
3	77000	−52±2 (ΔH)	201	1.7×10^{-1}
		−271±6 (ΔS)	213	3.5×10^{-2}
			223	9.4×10^{-3}
			232	3.0×10^{-3}
5	ca. 2(−40 °C)		233	4.2×10^{-1}
6	5800	−47±3 (ΔH)	204	6.7×10^{-1}
		−231±12 (ΔS)	212	2.1×10^{-1}
			218	1.3×10^{-1}
			222	7.0×10^{-2}
7	203000	−76±4 (ΔH)	220	1.2×10^{-1}
		−361±18 (ΔS)	228	2.3×10^{-2}
			230	1.9×10^{-2}
			238	5.9×10^{-3}
8[c]	2.6	−93±3 (ΔH)	291.0	4.7×10^{-1}
		−324±11 (ΔS)	293.0	3.8×10^{-1}
			295.6	2.6×10^{-1}
			298.0	1.9×10^{-1}
9[c]	27	−65±3 (ΔH)	283.0	9.8×10^{-2}
		−251±10 (ΔS)	288.0	5.3×10^{-2}
			293.0	3.7×10^{-2}
			298.0	2.1×10^{-2}
			303.0	1.6×10^{-2}
14[c,d]	ca. 2		293	ca. 5×10^{-1}
Hemerythrin[e]	ca. 2.2	−52 (ΔH)		
		−75 (ΔS)		

a) Standard state is 1 Torr at 20 °C. b) Extrapolated from ΔH and ΔS values. c) In acetonitrile. d) Ref. 10. e) Ref. 15.

nificant influence on the reactivity of cobalt complexes with O_2 as previously found for iron complexes.[9]

The dioxygen affinity of **7** is much lower than those of the Me_4-tpdp and Ph-tidp diiron complexes. Enthalpy change associated with oxygenation of **7** is −76 kJ mol^{-1}, which is significantly more negative (favorable) than those for the iron complexes (−47——−55 kJ mol^{-1}), whereas the loss in entropy (−361 J mol^{-1} K^{-1}) is significantly larger than those of the diiron complexes (−231——−274 J mol^{-1} K^{-1}). Highly unfavorable entropy change for **7** overcomes enthalpic stabilization, resulting in low dioxygen affinity for **7**. The observed enthalpy stabilization for **7** is partly ascribed to ligand field stabilization effect; for cobalt complexes, a high-spin Co(II) to low-spin Co(III) change occurs upon oxygenation, which provides a larger ligand field stabilization effect compared to iron complexes for which high-spin to low spin change does not occur. Such a highly favorable enthalpic stabilization is also found for the bpmp cobalt complexes. The stronger bonding contribution in ΔH associated with oxygenation of **7** (which involves both metal-dioxygen bond formation and an increment in metal-nitrogen bonding) seems to restrict molecular freedom, which leads to a decrease of entropy. Thus, the low dioxygen affinity observed for **7** compared to those of the Me_4-tpdp and Ph-tidp diiron complexes is partly attributable to an unfavorable entropy effect.

As found for diiron complexes, dioxygen affinity of the bpmp cobalt complexes containing a 2,6-bis(aminomethyl)-phenolate bridging skeleton is much higher than that of **7** with a 1,3-diamino-2-propanolate bridging one. Comparison of thermodynamic parameters of **7** and **9** is quite interesting. The enthalpy change for **9** is −65 kJ mol^{-1}, which is smaller than that for **7** (−76 kJ mol^{-1}), whereas the entropy change for **9** is −251 J mol^{-1} K^{-1}, which is significantly less negative (favorable) compared to that for **7** (−361 J mol^{-1} K^{-1}). Thus entropic stabilization derives a high dioxygen

affinity for **9**. For **8**, both enthalpic and entropic stabilization contributes to its high dioxygen affinity relative to that for **7**. Karlin et al. pointed out that dioxygen binding for synthetic copper-dioxygen complexes is as strong (enthalpically) as for biological O_2 carriers such as hemocyanin, but low dioxygen affinity for synthetic model compounds at room temperature is due to an unfavorable entropy effect.[31] Thus in order to synthesize dioxygen complexes which have high dioxygen affinity at room temperature, it seems to be essential to control the reaction entropy and the thermal stability against irreversible oxidation.

In the previous study, we succeeded in preparation of a diiron complex **14** which has a very high dioxygen affinity ($P_{1/2}$ = ca. 2 Torr at 20 °C in CH_3CN) which is comparable to that of Hr[15] and reasonable thermal stability (reversibility) at room temperature by using the dinucleating ligand, Ph-bimp, which has 2,6-bis(aminomethyl)phenolate bridging skeleton. Thus stereochemistry of dinucleating bridging skeleton is very important for controlling dioxygen affinity and thermal stability of the present type of dioxygen complexes. X-ray structures of the present type of dioxygen complexes reveal that the metal···metal separations are constrained to ca. 3.1—3.43 Å.[10,11,14b,14e] The metal–metal separations of the complexes with bpmp and Ph-bimp analogs which have a 2,6-bis(aminomethyl)phenolate bridging skeleton are in the wide range 3.14—4.13 Å, ([Fe_2(5-Me–HXTA)(μ-OH)(H_2O)$_2$], 3.137 Å;[32] [Fe_2(bpmp)($C_2H_5CO_2$)$_2$]$^+$, 3.365 Å;[33] [Cu_2(bpmp)Cl_2]$^+$, 4.13 Å[34]). This suggests that 2,6-bis(aminomethyl)phenolate bridging skeleton has a substantial structural flexibility for formation of a tribridged core with a peroxo bridge without significant steric constraint. The ligands containing 1,3-diamino-2-propanolate bridging skeleton tend to expand the metal–metal distance; the metal–metal distances of the complexes of tpdp or its analogs are constrained to be longer than 3.45 Å,[8,9,35] with a few exceptions, [Fe_2(NEt-HPTB)($OPPh_3$)$_2$(O_2)]$^{3+}$,[11] 3.43 Å; [Ni_2(Me_4-tpdp)(OMe)]$^{2+}$,[36] 3.01 Å. Such a stereochemical constraint seems to bring about a steric hindrance of a tribridged core upon oxygenation. The Fe–Fe separations of **1** and **5** are 3.59 and 3.68 Å, respectively. This may be responsible to the observed low dioxygen affinities for the complexes with 1,3-diamino-2-propanolate bridging skeleton relative to those for the complexes with 2,6-bis(aminomethyl)phenolate bridging skeleton.

Concluding Remarks

A series of diiron(II) complexes with various types of dinucleating ligands were prepared and their dioxygen affinities were measured for the first time. The results have provided some interesting insights into the thermodynamics for formation of dioxygen–diiron and –dicobalt complexes and their thermal stability against irreversible oxidation. Introduction of 4,5-diphenyl substituents into 2-imidazolyl group stabilized the thermal stability of μ-peroxo diiron species against irreversible oxidation as well as 6-methyl substituent into 2-pyridyl group. Those substituents appear to weaken the electron donor ability of dinucleating ligand to stabilize the divalent oxidation state of iron and to form a hydrophobic cavity for a O_2 binding site, which would suppress the irreversible oxidation and facilitate the reversible oxygenation. Within a series of diiron(II) complexes with the same dinucleating ligand, dioxygen affinity is well correlated with electron donor ability of bridging carboxylates, although the ΔH and ΔS variations in these complexes are random. In contrast to the above trend, the Ph-tidp complexes provide lower dioxygen affinity relative to the Me_4-tpdp complexes whose electron donor abilities are weaker than those of the Ph-tidp complexes. Dicobalt complexes are substantially less reactive than diiron complexes with the same dinucleating ligand. This is probably due to high redox potential of cobalt complexes. Significant enhancement of dioxygen affinity was observed for both iron and cobalt complexes with 2,6-bis(aminomethyl)phenolate bridging skeleton compared to the complexes with a 1,3-diamino-2-propanolate bridging one. Thermodynamic study of cobalt complexes suggests that the observed enhancement is mainly attributable to favorable entropy effect. For a fuller understanding of the variations in dioxygen affinity and thermal stability against irreversible oxidation observed for the present type of dinuclear complexes, further systematic structural and thermodynamic studies are required.

Financial supports by a Grant-in-Aid for Scientific Research for Priority Area "Molecular Biometallics" from the Ministry of Education, Science, Sports and Culture are acknowledged.

References

1) L. Que, Jr., in "Bioinorganic Catalysis," ed by J. Reedijk, Marcel Dekker Inc., Amsterdam (1993), pp. 347—393; A. L. Feig and S. J. Lippard, *Chem. Rev.*, **94**, 759 (1994).

2) P. C. Wilkins and R. G. Wilkins, *Coord. Chem. Rev.*, **79**, 195 (1987); R. E. Stenkamp, *Chem. Rev.*, **94**, 715 (1994).

3) B.-M. Sjöberg and A. Gräslund, *Adv. Inorg. Chem.*, **5**, 87 (1983); P. Nordlund, B.-M. Sjöberg, and H. Eklund, *Nature*, **345**, 593 (1990); J. M. Bollinger, Jr., W. H. Tong, N. Ravi, B. H. Huynh, D. E. Edmondson, and J. Stubbe, *J. Am. Chem. Soc.*, **116**, 8024 (1994).

4) A. C. Rosenzweig, P. Nordlund, P. M. Takahara, C. A. Frederick, and S. J. Lippard, *Chem. Biol.*, **2**, 409 (1995); B. J. Wallar and J. D. Lipscomb, *Chem. Rev.*, **96**, 2625 (1996).

5) K. E. Liu, A. M. Valentine, D. Qiu, D. E. Edmondson, E. H. Appelman, T. G. Spiro, and S. J. Lippard, *J. Am. Chem. Soc.*, **117**, 4997 (1995).

6) S.-K. Lee, J. C. Nesheim, and J. D. Lipscomb, *J. Biol. Chem.*, **268**, 21569 (1993); L. Shu, J. C. Nesheim, K. Kauffmann, E. Münk, J. D. Lipscomb, and L. Que, Jr., *Science*, **275**, 515 (1997), and references cited therein.

7) a) N. Kitajima, H. Fukui, Y. Moro-oka, Y. Mizutani, and T. Kitagawa, *J. Am. Chem. Soc.*, **112**, 6402 (1990); b) N. Kitajima, N. Tamura, H. Amagai, H. Fukui, Y. Moro-oka, Y. Mizutani, T. Kitagawa, R. Mathur, K. Heerwegh, C. A. Reed, C. R. Randall, L. Que, Jr., and K. Tatsumi, *J. Am. Chem. Soc.*, **116**, 9071 (1994).

8) a) S. Ménage, B. A. Brennan, C. Juarez-Garcia, E. Münck, and L. Que, Jr., *J. Am. Chem. Soc.*, **112**, 6423 (1990); b) Y. Dong,

S. Ménage, B. A. Brennan, T. E. Elgren, H. G. Jang, L. L. Pearce, and L. Que, Jr., *J. Am. Chem. Soc.*, **115**, 1851 (1993).

9) a) Y. Hayashi, M. Suzuki, A. Uehara, Y. Mizutani, and T. Kitagawa, *Chem. Lett.*, **1992**, 91; b) Y. Hayashi, T. Kayatani, H. Sugimoto, M. Suzuki, K. Inomata, A. Uehara, Y. Mizutani, T. Kitagawa, and Y. Maeda, *J. Am. Chem. Soc.*, **117**, 11220 (1995).

10) T. Ookubo, H. Sugimoto, T. Nagayama, H. Masuda, T. Sato, K. Tanaka, Y. Maeda, H. Okawa, Y. Hayashi, A. Uehara, and M. Suzuki, *J. Am. Chem. Soc.*, **118**, 701 (1996).

11) Y. Dong, S. Yan, V. G. Young, and L. Que, Jr., *Angew. Chem., Int. Ed. Engl.*, **35**, 618 (1996).

12) K. Kim and S. J. Lippard, *J. Am. Chem. Soc.*, **118**, 4914 (1996).

13) Abbreviations of ligands: HB(3,5-*i*Pr$_2$Pz)$_3$ = hydrotris(3,5-diiso-propyl-4-pyrazolyl)borate; *N*-Et-HPTB = *N*,*N*,*N*′,*N*′-tetrakis-[(1-ethyl-2-benzimidazolyl)methyl)-1,3-diamino-2-propanolate; Ph-bimp = 4-methyl-2,6-bis{*N*,*N*-bis[(1-methyl-4,5-diphenyl-2-imidazolyl)methyl]aminomethyl}phenolate; bimp = 4-methyl-2,6-bis{*N*,*N*-bis[1-methyl-2-imidazolyl)methyl]aminomethyl}phenolate; bzimp = 2,6-bis{[*N*,*N*-bis(2-benzimidazolylmethyl)amino]-methyl}-4-methylphenolate.

14) a) M. Suzuki, H. Kanatomi, and I. Murase, *Chem. Lett.*, **1981**, 1745; b) M. Suzuki, I. Ueda, H. Kanatomi, and I. Murase, *Chem. Lett.*, **1983**, 185; c) M. Suzuki, H. Kanatomi, and I. Murase, *Bull. Chem. Soc. Jpn.*, **57**, 36 (1984); d) M. Suzuki, T. Sugisawa, and A. Uehara, *Bull. Chem. Soc. Jpn.*, **63**, 1115 (1990); e) K. Kayatani, Y. Hayashi, M. Suzuki, and A. Uehara, *Bull. Chem. Soc. Jpn.*, **67**, 2980 (1994).

15) G. B. Jameson and J. A. Ibers, in "Bioinorganic Chemistry," ed by I. Bertini, H. B. Gray, and S. J. Lippard, University Science Books, Sausalito (1994), p. 167, and references cited therein.

16) H. Bredereck and G. Theilig, *Chem. Ber.*, **86**, 88 (1953).

17) N. J. Rose and R. S. Drago, *J. Am. Chem. Soc.*, **81**, 6138 (1959); J. P. Collman, J. I. Brauman, K. M. Doxsee, T. R. Halbert, S. E. Hayes, and K. S. Suslick, *J. Am. Chem. Soc.*, **100**, 2761 (1978).

18) C. A. McAuliffe, H. F. Al-Khateeb, D. S. Barratt, J. C. Briggs, A. Challita, A. Hosseiny, M. G. Little, A. G. Mackie, and K. Minten, *J. Chem. Soc., Dalton Trans.*, **1983**, 2147.

19) Deposited as Document No. 71051 at the Office of the Editor of Bull. Chem. Soc. Jpn.

20) G. M. Sheldrick, "SHELXS-86. A Program for Crystal Structure Determination," University of Göttingen, FRG (1986).

21) P. T. Beurskens, G. Admiraal, G. Beurskens, W. P. Bosman, R. de Gelder, R. Israel, and J. M. M. Smits, "The DIRDIF-94 Program System, Technical Report of the Crystallography Laboratory," University of Nijmegen, The Netherlands (1994).

22) M. Suzuki, et al., To be submitted.

23) M. S. Mashuta, R. J. Webb, J. K. McCusker, E. A. Schmitt, K. J. Oberhausen, J. F. Richardson, R. M. Buchanan, and D. N. Hendrickson, *J. Am. Chem. Soc.*, **114**, 3815 (1992).

24) R. C. Reem and E. I. Solomon, *J. Am. Chem. Soc.*, **109**, 1216 (1987).

25) M. Suzuki, H. Oshio, A. Uehara, K. Endo, M. Yanaga, S. Kida, and K. Saito, *Bull. Chem. Soc. Jpn.*, **61**, 3907 (1988).

26) M. Ciampolini and I. Bertini, *J. Chem. Soc. A*, **1961**, 2241.

27) A. K. Shiemke, T. M. Loehr, and J. Sanders-Loehr, *J. Am. Chem. Soc.*, **106**, 4951 (1984).

28) A. B. P. Lever and H. B. Gray, *Acc. Chem. Res.*, **11**, 348 (1978).

29) R. D. Jones, D. A. Summerville, and F. Basolo, *Chem. Rev.*, **79**, 139 (1979), and the references cited therein.

30) E. C. Niederhoffer, J. H. Timmons, and A. E. Martell, *Chem. Rev.*, **84**, 137 (1984), and the references cited therein.

31) K. D. Karlin, S. Kaderli, and A. D. Züberbühler, *Acc. Chem. Res.*, **30**, 139 (1997).

32) B. P. Murch, F. C. Bradley, P. D. Boyle, V. Papaefthymiou, and L. Que, Jr., *J. Am. Chem. Soc.*, **109**, 7993 (1987).

33) A. S. Borovik, V. Papaefthymiou, L. F. Taylor, O. P. Anderson, and L. Que, Jr., *J. Am. Chem. Soc.*, **111**, 6183 (1989).

34) Y. Nishida, H. Shimo, H. Maehara, and S. Kida, *J. Chem. Soc., Dalton Trans.*, **1985**, 1945.

35) D. L. Jameson, C. L. Xie, D. N. Hendrickson, J. A. Potenza, and H. J. Schugar, *J. Am. Chem. Soc.*, **109**, 740 (1987); Q. Chen, J. B. Lynch, P. G. Romero, A. B. Hussein, G. B. Jameson, C. J. O'Conner, and L. Que, Jr., *Inorg. Chem.*, **27**, 2673 (1988); M. Suzuki, T. Sugisawa, H. Senda, H. Oshio, and A. Uehara, *Chem. Lett.*, **1989**, 1091; M. Suzuki, H. Senda, M. Suenaga, T. Sugisawa, and A. Uehara, *Chem. Lett.*, **1990**, 923; S. Kawata, M. Nakamura, Y. Yamashita, K. Asai, K. Kikuchi, I. Ikemoto, M. Katata, and H. Sano, *Chem. Lett.*, **1992**, 135.

36) K. Yamaguchi, S. Koshino, F. Akagi, M. Suzuki, A. Uehara, and S. Suzuki, *J. Am. Chem. Soc.*, **119**, 5752 (1997).